Proceedings of the Canadian Society for Mechanical Engineering International Congress
32nd Annual Conference of the Computational Fluid Dynamics Society of Canada
Canadian Society of Rheology Symposium
CSME/CFDSC/CSR 2025
May 25–28, 2025, Montréal, Québec, Canada

NUMBER

Characterization of flow curvature effects on a NACA 0015 airfoil attached at the quarter-chord

Philippe Rochefort[1], Louis Précourt[1], Grégoire Winckelmans[2], Guy Dumas[1*]

[1]LMFN CFD laboratory, Mechanical Engineering Department, Université Laval, Quebec, Canada
[2]Institute of Mechanics, Materials and Civil Engineering (iMMC), Université catholique de Louvain (UCLouvain), Louvain-la-Neuve, Belgium
[*]gdumas@gmc.ulaval.ca

DATE

***Abstract*—**The blades of vertical-axis turbines (VAT) operate in curved and nearly circular flow. Compared to a uniform flow, the curved streamlines alter the aerodynamic coefficients of the airfoil. As a result, measuring and predicting the aerodynamic coefficients of an airfoil in curved flow presents a challenge. In this work, we first present a methodology to properly measure the aerodynamic coefficients (lift, drag, and moment) of a NACA 0015 airfoil attached at the quarter-chord in steady curved flow at $Re_c = 6 \times 10^6$ using CFD with a "key-hole mesh domain". By varying the airfoil's angle of attack and the airfoil's chord to turbine's radius ratio (c/R), the curves for $C_l(\alpha)$, $C_{m_{c/4}}(\alpha)$ and $C_d(\alpha)$ are obtained and presented. The results show that the curvature effects on the aerodynamic coefficients are significant. In particular, it is observed that the drag is significantly influenced by the flow curvature, which we show to be closely related to the moment coefficient of the airfoil and the moment coefficient about the airfoil's rotation axis (C_{m_0}). Furthermore, the Coriolis effect on C_d is shown to cause an asymmetry in the typical U-shaped drag curve observed in uniform flow. The findings of this investigation will help develop improved models for actuator line methods (ALM).

***Keywords-component*—Flow curvature; aerodynamic coefficents; vertical-axis turbine; computational fluid dynamics**

I. INTRODUCTION

The Actuator Line Method (ALM) is a moderate-fidelity model used to predict the aerodynamic performance of wind or water turbines and to accurately replicate their wake behavior. This method, initially introduced by Sørensen and Shen [1], replaces the body-meshed lifting surface with equivalent volume forces in the Navier-Stokes equations. These forces are calculated for each blade section by estimating a local upstream velocity and angle of attack, and by using previously computed aerodynamic airfoil coefficients. This method allows for bypassing the resolution of the actual boundary layers of the lifting surface. Thus, it significantly reduces the mesh size and computing cost. The method is increasingly applied in the study of wind turbine, particularly for axial flow turbine, as it was shown to be effective in accurately replicating realistic performances [2] and capturing the correct wake behavior [3].

Regarding vertical-axis turbines (VAT), there are challenges in modeling them with the ALM. As mentioned in the work of Mohamed et al. [4], the primary challenge in VAT modeling using the ALM is the quality of the airfoil's aerodynamic coefficients data. Specifically, the blade of this type of turbine operates in a curved and unsteady flow. These two characteristics of the flow alters the aerodynamic coefficients compared to those in uniform and stationary flow. Since the ALM requires the appropriate aerodynamic coefficients to accurately replicate the forces exerted by the blade on the flow, it is crucial that the aerodynamic coefficients used by the ALM account for those effects. In this paper, we focus on the impact of flow curvature while leaving the analysis of unsteady effects for future work. Thus, flow curvature will be treated as a steady phenomenon, as discussed in Section II-A, and is characterized by the parameter c/R, where c is the airfoil's chord length and R the radius of the H-Darrieus turbine with straight blades.

In this context, the effects of flow curvature were first studied by Migliore and Wolfe [5]. In their work, they discuss the effects of curvature using the concepts of "virtual camber"and "virtual incidence". They demonstrated that the aerodynamics of a symmetric airfoil in curved flow can be analogous to the aerodynamics of a cambered airfoil with a non-zero incidence in uniform flow. They arrived at this conclusion through a purely geometric transformation, which allows for modification of the airfoil profile by converting the curved flow into a uniform flow, thus unfolding the theoretical

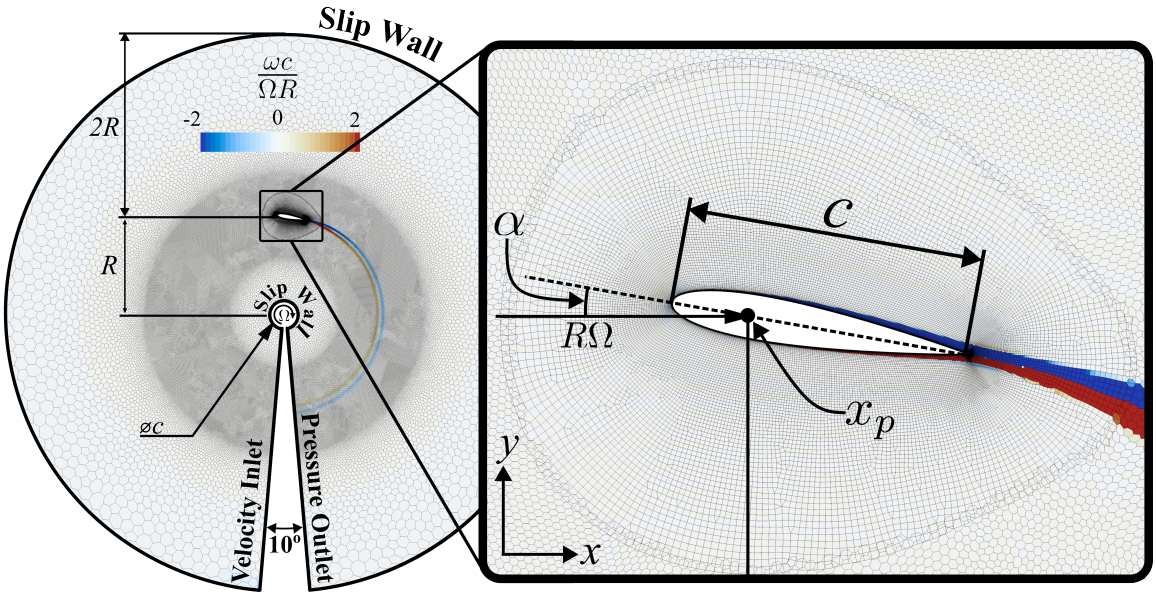

Figure. 1. Boundary conditions and key-hole mesh domain setup for the simulation of a NACA0015 airfoil in curved flow with a $c/R = 2/7$. The attachment point on the airfoil is located at the quarter-chord ($x_p/c = 0.25$) and the angle $\alpha = 10^o$. A zoomed-in view of the airfoil is also provided, highlighting the important parameters, the body-fitted mesh around the airfoil and the normalized vorticity field.

curved streamlines while preserving the local angles between the streamlines and the surface of the airfoil. An example of this methodology is illustrated in Fig. 3 of this work.

Rainbird [6] and Bianchini [7] demonstrated the effects of virtual camber and virtual incidence with comparisons of experimental results of an airfoil in uniform flow with a camber similar to the virtual camber of a symmetric airfoil in curved flow, with CFD results of a symmetric airfoil in rotation. However, in these papers, the airfoil's quarter-chord moment coefficient ($C_{m_{c/4}}$) was not evaluated and was only briefly discussed. Yet, the quarter-chord moment coefficient is also affected by the curvature effects and plays a significant role on the total torque coefficient at the center of rotation of the VAT (C_{m_0}), which is proportional to the power coefficient. Therefore, one objective of the present paper is to characterize and analyze these two moment coefficients in the context of an airfoil in pure rotation. We will show their fundamental relationship with the airfoil's drag coefficient.

Thus, this work does not aim to generate a database of aerodynamic coefficients in curved flow but rather to provide the physical basis on which proper flow curvature corrections could be developed for the aerodynamic polars used in the ALM modelling of VAT where the blades experience flow curvature effects (yet are not operating in pure rotation).

II. Methodology

A. Problem description

The studied problem is based on a 2D one-bladed vertical-axis turbine. In the reference frame of the airfoil, the flow is curved due to the rotation of the airfoil. It is this curvature that modifies the aerodynamic coefficients of the airfoil. However, the curvature of the flow is not perfectly circular due to the upstream velocity. In fact, the upstream velocity modifies the actual flow curvature at every instant over the rotation cycle of the airfoil. We will neglect the modification of the flow curvature caused by the upstream velocity. This is left for future work. Thus, the resulting flow in the reference frame of the airfoil is a circular curved flow, as if the airfoil was undergoing circular rotation without upstream velocity. In this case of curvature, steady-state simulations with a circular curved flow can be used to study the effects of curvature on the aerodynamic coefficient curves of an airfoil. According to the coordinates system in the zoom around the airfoil in Fig. 1, the aerodynamic coefficients studied are the lift coefficient (C_l), defined in the y direction, the quarter-chord moment coefficient ($C_{m_{c/4}}$), defined positive in the clockwise direction and the drag coefficient (C_d), defined in the x direction.

The problem studied involves investigating the effects of curvature on the aerodynamic coefficient curves of an airfoil in a circular curved flow, with a chord-based Reynolds number (Re) of $6 \cdot 10^6$ (high enough to assume fully-turbulent boundary layers) and the flow is considered incompressible for all simulations. It should also be noted that although VATs often operate at lower Reynolds numbers, curvature effects themselves are not expected to be Re-dependent. In curved flow, the Reynolds number is defined using the theoretical velocity at the turbine's radius, which is the angular velocity (Ω) multiplied by the turbine's radius (R) as shown in Fig. 1. The coefficient curves are obtained by varying the angle α, which is the angle between the airfoil and the curved streamlines at the quarter-chord as depicted in the zoomed-in view of the airfoil in Fig. 1. This location was chosen because it corresponds to the aerodynamic center of thin airfoils in

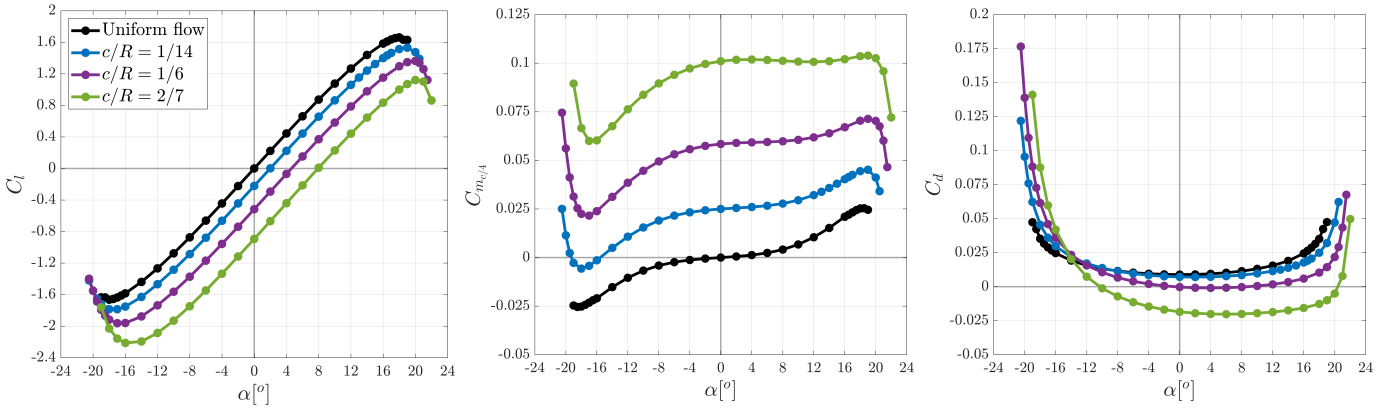

Figure. 2. Comparison between the values of C_l, C_d and $C_{m_{c/4}}$ obtained from CFD simulations for a NACA0015 airfoil in uniform flow (black) and in curved flow with $c/R = 1/14$ (blue), $c/R = 1/6$ (purple) and $c/R = 2/7$ (green).

uniform flow and it would be the effective angle of attack used in the ALM. This allows us to consider the measured x and y-forces as the lift and drag. The flow curvature is controlled by the c/R ratio. A smaller ratio results in less curvature, while a larger ratio leads to greater curvature.

B. Numerical methodology

The steady-state Reynolds averaged Navier-Stokes (RANS) equations are solved using the commercial finite-volume solver Siemens® STAR-CCM+®. A segregated approach with the SIMPLE algorithm is employed for the pressure-velocity coupling with second-order schemes for all flow variables. The turbulence is modeled using the Spalart-Allmaras turbulence model with curvature correction enabled [8, 9]. The curvature effects are not expected to be dependent on the turbulence model. Even though there are small discrepancies on the aerodynamic coefficients between turbulence models, the trends induced by curvature effects should remain consistent.

C. Domain and mesh

To obtain a circular curved flow, a key-hole mesh domain is used as shown in Fig. 1. This type of domain was initially presented by Akimoto et al. [10] to validate a conformal mapping method that transforms a curved flow to a uniform flow to predict the aerodynamic coefficients of an airfoil in curved flow. The method demonstrated good prediction accuracy for the studied cases, but only two different angles α were studied and the c/R ratio was kept at 0.2. In the present work, we vary both the angle α and the c/R ratio to study the effect of curvature on the aerodynamic coefficient curves. The advantage of the key-hole mesh domain is that it allows the wake to exit through the outlet, ensuring a clean flow at the inlet. The circular flow is defined in STAR-CCM+ using a reference frame that allows to define the airfoil's rotational motion relative to the inertial frame of reference. This rotating reference frame is defined with the angular velocity of the blade (Ω). For the turbulent boundary conditions, a turbulent viscosity ratio of $\nu_t/\nu = 0.02$, corresponding to a clean flow, is imposed at the inlet. A zero normal velocity (u) is imposed at the inlet, and a uniform reference static pressure (p_{static}) is imposed at the outlet, both being the values in the inertial reference frame. Indeed, the implemented "rotating frame simulation setup"ensures a velocity profile corresponding to solid body rotation. Furthermore, the increased pressure generated by the centrifugal term is also accounted for by Star-CCM+ within the rotating reference frame. Thus, the velocity (u_{rel}) and pressure profiles (p_{rel}) in the rotating reference frame are those of a curved circular flow corresponding to solid body rotation as expressed in Eqs. (1) and (2).

$$u_{\text{rel}} = u + \Omega r = \Omega r \tag{1}$$

$$p_{\text{rel}} = p_{\text{static}} + \frac{1}{2}\Omega^2 r^2 \tag{2}$$

Finally, the boundary conditions on the inner and outer circular boundaries are set to slip walls.

The mesh, composed of polygonal cells, has two levels of mesh refinement. Near wall resolution is achieved using prism layers, a value of $y^+ \simeq 1$ and a maximum normal growth rate of 1.2 to ensure proper boundary layer resolution. The mesh around the blade for near wall resolution consists of 36,209 cells. An additional refinement level in a circular band is used to properly resolve the flow around the airfoil and its wake as shown in Fig. 1, bringing the total background mesh to 109,897 cells. It has also been verified that the results presented in this work are mesh-independent. Moreover, the results have not been validated against experimental data due to the lack of adequate experimental results in the literature. Indeed, the circular flow makes experimental force measurements on an airfoil challenging especially in terms of the pitching moment [11].

III. Results and Discussion

This section presents the curvature effects on the aerodynamic coefficients of the airfoil. The graphs of the coefficient curves for different levels of curvature are shown in Fig. 2.

A. Effects on C_l

The effect on the lift coefficient is addressed first. Fig. 2 shows that as the curvature increases, the lift coefficient decreases and the curve shifts to the right. Thus, for a

given angle α, the lift coefficient decreases as the curvature increases. This can be explained by the concept of virtual camber. As mentioned in Section I, a symmetric airfoil in curved flow can be considered analogous to a cambered airfoil in uniform flow as shown in Fig. 3. This figure was obtained using the geometric transformation presented in the works of Migliore and Wolfe [5] for the present case, namely a NACA 0015 airfoil in rotation with $c/R = 2/7$. In this case, the virtual camber is a negative camber, which results in the lift coefficient curve shifting to the right. Thus, the higher the curvature, the greater the negative virtual camber, and the further the lift coefficient curve shifts to the right, as can be observed in Fig. 2.

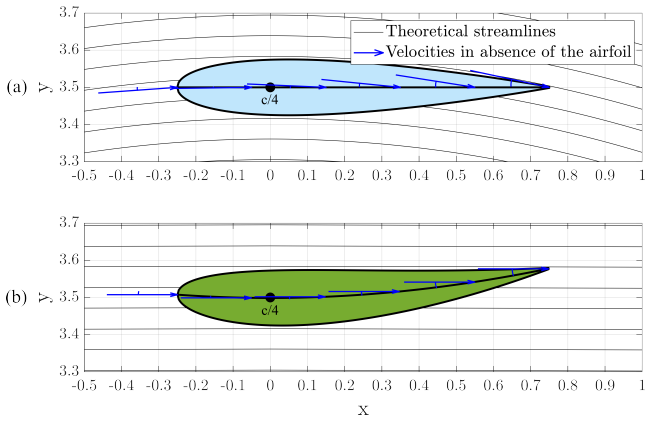

Figure. 3. Comparison of (a): a symmetric NACA 0015 airfoil in curved flow with a $c/R = 2/7$ ratio, to its analogous case (b): a modified airfoil with negative camber in uniform flow, illustrating the virtual camber concept.

Fig. 4 shows the pressure distribution for the cases of uniform flow and curved flow ($c/R = 2/7$) at $\alpha = 0^o$. This figure confirms that the curved flow generates a loading distribution very similar to that of a negatively cambered airfoil as suggested above. In particular, one notices the shift of the stagnation point on the upper surface near the leading edge.

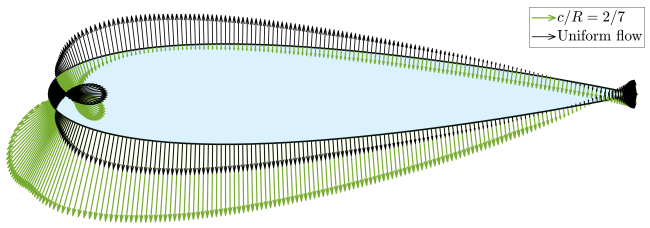

Figure. 4. Pressure coefficient distribution over the airfoil for $\alpha = 0^o$ in curved flow with $c/R = 2/7$ (green) and in uniform flow (black).

As shown by Fig. 4, it is possible to confirm that the loading along the entire airfoil surface is affected, compared to the distribution in uniform flow. This explains why the C_l in curved flow is notably negative, as shown in Table I.

B. Effects on $C_{m_{c/4}}$

For the effect on $C_{m_{c/4}}$, as the curvature increases, the $C_{m_{c/4}}$ values become more positive (clockwise).

TABLE. I
AERODYNAMIC COEFFICIENTS FOR $\alpha = 0^o$ IN UNIFORM AND CURVED FLOW

Flow	C_l	C_d	$C_{m_{c/4}}$
Uniform	0.000	0.009	0.000
Curved ($c/R = 2/7$)	-0.893	-0.018	0.101

Once again, an explanation for this effect is the virtual camber shown in Fig. 3, as having a negative camber also results in more positive $C_{m_{c/4}}$. Indeed, a negative camber enhances a negative loading from the quarter-chord to the trailing edge of the airfoil, which leads to a greater positive moment at the quarter-chord. This effect is clearly visible in Fig. 4. The enhanced negative loading from the quarter-chord to the trailing edge generates a lever arm, creating a positive moment at the quarter-chord. This is also confirmed by the values of $C_{m_{c/4}}$ shown in Table I.

C. Effects on C_d

Regarding the effects of curvature on the drag coefficient, the C_d graph in Fig. 2 shows that as the curvature increases, the C_d curves decrease for positive angles of attack and slightly shift to the right. As observed in the graph by the curves $c/R = 1/6$ and $c/R = 2/7$, the values of C_d can even become negative. This, of course, cannot be explained with the analogy of a negative virtual camber since the C_d of a cambered airfoil always remains positive ($C_d > 0$).

The negative C_d may seem surprising, but the results are physically valid when considering the physical requirement on the coefficient of total torque about the airfoil's rotation axis (C_{m_0}). Considering an airfoil in rotation attached to an arm with no upstream velocity, as in the problem studied here (pure rotation), it would require torque and thus energy to rotate the airfoil. In other words, there must be a resistance to rotate the airfoil. Thus, as illustrated in the diagram in Fig. 5, the only physical requirement is that C_{m_0} must be positive (clockwise) to represent this resistance that one should compensate to make the airfoil rotate in the anti-clockwise direction. From the

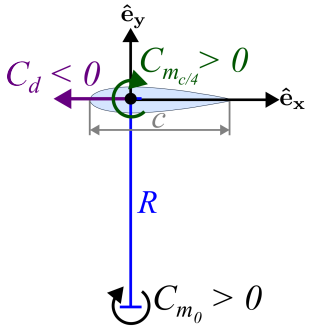

Figure. 5. Forces and moments diagram of the rotating airfoil attached at $c/4$. The physical criterion for the total moment coefficient about the rotation axis (in black) is depicted at the rotation axis, while the negative C_d (in purple) and the positive $C_{m_{c/4}}$ (in green) are also illustrated at the quarter chord.

diagram in Fig. 5, it can also be noted that C_{m_0} is generated by the lever arm created by C_d and $C_{m_{c/4}}$. The equation of the physical requirement to be satisfied is expressed in Eq. (3).

$$C_{m_0} = C_d \frac{R}{c} + C_{m_{c/4}} > 0 \tag{3}$$

Therefore, it is possible to satisfy the physical requirement with a negative C_d if Eq. (4) is respected.

$$C_{m_{c/4}} > -C_d \frac{R}{c} \tag{4}$$

The graph in Fig. 6 confirms that $C_{m_0} > 0$ is satisfied for all α for the curvature $c/R = 2/7$. This means that having a negative drag is physically valid. Furthermore, Fig. 6 also

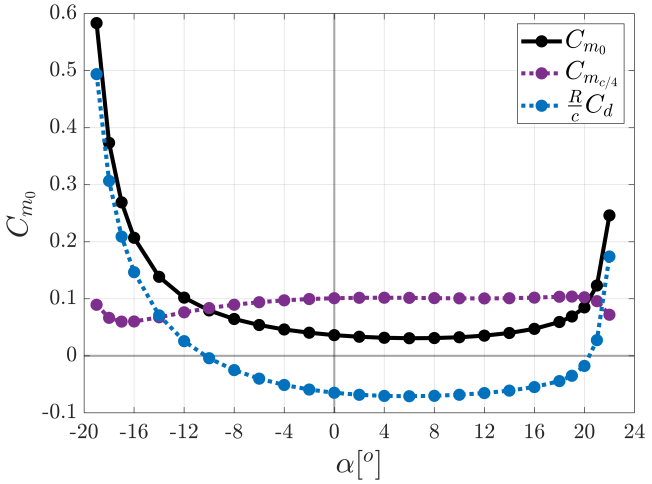

Figure. 6. C_{m_0} (black) in curved flow with $c/R = 2/7$ as a function of α and its contributions : $C_{m_{c/4}}$ (purple) and $C_d \frac{R}{c}$ (blue).

shows the strong relationship between $C_{m_{c/4}}$ and C_d when an airfoil is attached to an arm in a curved flow. Another important conclusion that can be drawn from this analysis using Eq. (3) and the concept of the center of pressure (x_{cp}), where $C_m = 0$, is that when the airfoil is attached at x_{cp}, the resistance generated by C_{m_0} is solely attributable to C_d. In fact, when the airfoil is attached at x_{cp}, (3) simplifies to (5).

$$C_{m_0} = C_d \frac{R}{c} > 0 \tag{5}$$

We can conclude that C_d is always positive when the airfoil is attached at its center of pressure. Finally, the details of the analysis presented above aim to illustrate the fundamental relationship between C_{m_0}, the tangential force (or C_d when referenced to $c/4$) and the C_m at the attachment point. Also, it is important to understand that the attachment point also has a significant effect on the values of the aerodynamic coefficients.

With the pressure coefficient (C_p) distributions on the airfoil for $\alpha = 0^o$ shown in Fig. 4, we can see how a negative drag can be produced by the significant suction at the leading edge in curved flow. This difference in suction may be attributed to the displacement of the stagnation point in curved flow, that can be observed from the dividing streamline shown as the black dashed line in both cases presented in Fig. 7. This shift increases the curvature of the streamlines at the leading edge. Indeed, it can be observed in Fig. 7 that the streamlines in curved flow exhibit greater curvature near the leading edge, and, as described by the term associated to the centrifugal force in the Navier-Stokes equations ($\rho \frac{V_\theta^2}{r} = \frac{\partial p}{\partial r}$), a higher curvature of the streamlines increases the normal pressure gradient, shown in black in Fig. 7 (b), leading to increased suction at the leading edge. Thus, since the uniform and curved

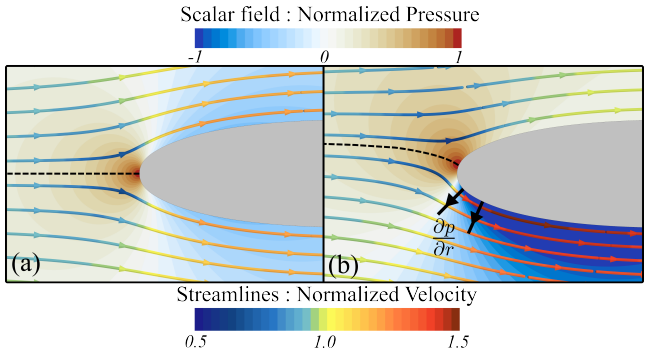

Figure. 7. Pressure coefficient field superposed with the streamlines for cases (a) uniform flow and (b) curved flow with $c/R = 2/7$ at $\alpha = 0^o$.

flow cases have the same reference pressure, but the pressure at the leading edge of the airfoil in curved flow is lower due to the greater curvature of the streamlines, a larger suction is created, which results in a negative C_d, as shown in Table I.

Another interesting point to further analyze how C_d decreases in curved flow is to examine the pressure (C_{d_p}) and friction (C_{d_f}) contributions of C_d, as shown in Fig. 8 for the cases of uniform flow and curved flow with $c/R = 2/7$.

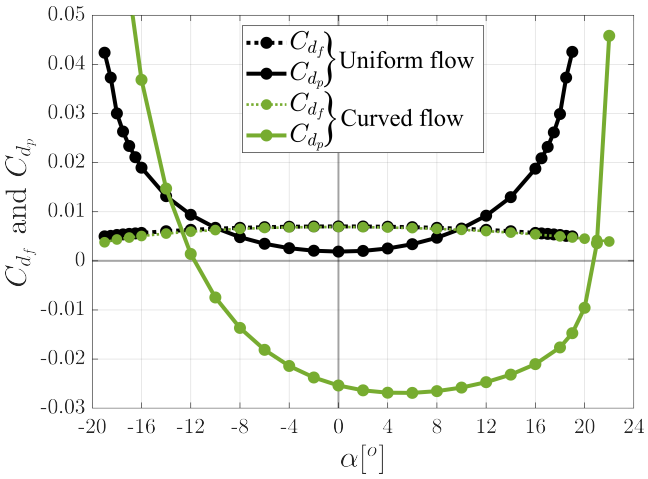

Figure. 8. Friction drag (dashed line) and pressure drag (solid line) coefficients in uniform flow (black) and in curved flow with $c/R = 2/7$ (green).

With this graph, we conclude that only C_{d_p} is affected, and it is this contribution that makes the C_d negative. Moreover, C_{d_f} in both uniform and curved flow is similar. Therefore, the C_{d_f} is essentially not affected by the curved flow.

Finally, it is possible to explain the cause of the shift of the C_d curve to the right, which can be visualized in Fig. 2, with

the Coriolis force. In a rotating frame, two additional inertial terms are considered: the centrifugal force and the Coriolis force. In our case, in cylindrical coordinates, the centrifugal force acts in the radial direction, which can be assimilated to the y-direction, and the Coriolis force acts in both the radial and theta directions, where the θ direction can be approximated by the x-direction. Therefore, one can argue that the Coriolis force has an influence on the C_d of the airfoil. Fig. 9 shows

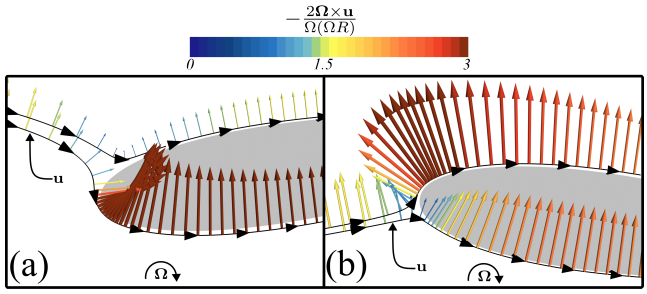

Figure. 9. Coriolis force vectors on two streamlines (in black) near the leading edge of the airfoil in curved flow with $c/R = 2/7$. (a): $\alpha = -8^o$ and (b): $\alpha = 8^o$.

the effect of the Coriolis force on two streamlines near the airfoil. For negative α, it can be seen that the Coriolis effect at the leading edge creates an overpressure, which increases C_d. Whereas, for positive α, the Coriolis effect at the leading edge creates suction, which reduces C_d. This effect can be visualized in Fig. 2 by the asymmetry of the C_d curve (which exhibits a U-shape in a uniform flow). Since C_d is decreased for positive angles and increased for negative angles due to the Coriolis effect, the C_d curve shifts to the right.

IV. Conclusion

The effects of curvature have been studied on a NACA 0015 airfoil by varying the c/R ratio of a purely rotational flow. The results are presented in the form of aerodynamic coefficient curves ($C_l(\alpha)$, $C_d(\alpha)$, $C_{m_{c/4}}(\alpha)$). These results confirm that the flow curvature significantly modifies the coefficients compared to those in uniform flow. Aerodynamic polars must thus be adapted to properly include the curvature effects and these effects depend on the attachment point of the airfoil. The effect on C_l and $C_{m_{c/4}}$ is shown to be equivalent to a negative camber, while the effect on C_d is more intricate. It is seen that C_d can be negative, as it is fundamentally linked to $C_{m_{c/4}}$ and the total moment coefficient about the rotation axis (C_{m_0}), representing the forces-moment system of the turbine. Finally, the results will also be used to develop and validate corrections for the curvature effects in the context of H-Darrieus turbine simulations. A paper on these corrections in an ALM method is currently in preparation.

Acknowledgment

Financial support from the Natural Sciences and Engineering Reasearch Council of Canada (NSERC), the Fonds de recherche du Québec secteur Nature et technologies (FRQNT) and the Régie de l'énergie du Québec is gratefully acknowledged along with the computational resources provided by the Digital Reasearch Alliance of Canada.

References

[1] W. Z. Shen, J. H. Zhang, and J. N. Sørensen, "The actuator surface model: A new Navier–Stokes based model for rotor computations," *Journal of Solar Energy Engineering*, vol. 131, 011002, 2009.

[2] F. Trigaux, P. Chatelain, and G. Winckelmans, "Investigation of blade flexibility effects on the loads and wake of a 15 mw wind turbine using a flexible actuator line method," *Wind Energy Science*, vol. 9, pp. 1765–1789, 2024.

[3] S. Richard, L. A. Martinez-Tossas, and C. Meneveau, "Comparison of wind farm large eddy simulations using actuator disk and actuator line models with wind tunnel experiments," *Renewable Energy*, vol. 116, pp. 470–478, 2018.

[4] O. S. Mohamed, P. F. Melani, F. Balduzzi, G. Ferrara, and A. Bianchini, "An insight on the key factors influencing the accuracy of the actuator line method for use in vertical-axis turbines: Limitations and open challenges," *Energy Conversion and Management*, vol. 270, 116249, 2022.

[5] P. G. Migliore, W. P. Wolfe, and R. E. Walters, *The effects of flow curvature on the aerodynamics of Darrieus wind turbines*. Morgantown, West Virginia: Dept. of Aerospace Engineering, West Virginia University, 1980.

[6] J. M. Rainbird, A. Bianchini, F. Balduzzi, J. Peiró, J. M. R. Graham, G. Ferrara, and L. Ferrari, "On the influence of virtual camber effect on airfoil polars for use in simulations of darrieus wind turbines," *Energy Conversion and Management*, vol. 106, pp. 373–384, 2015.

[7] A. Bianchini, F. Balduzzi, G. Ferrara, and L. Ferrari, "Virtual incidence effect on rotating airfoils in darrieus wind turbines," *Energy Conversion and Management*, vol. 111, pp. 329–338, 2016.

[8] P. R. Spalart and S. R. Allmaras, "A one-equation turbulence model for aerodynamic flows," *La Recherche Aérospatiale*, vol. 1, pp. 5 – 21, 1994.

[9] P. R. Spalart and M. Shur, "On the sensitization of turbulence and models to rotation and curvature," *Aerospace Science and Technology*, vol. 5, pp. 297–302, 1997.

[10] H. Akimoto, Y. Hara, T. Kawamura, T. Nakamura, and Y.-S. Lee, "A conformal mapping technique to correlate the rotating flow around a wing section of vertical axis wind turbine and an equivalent linear flow around a static wing," *Environmental Research Letters*, vol. 8, 044040, 2013.

[11] K. Ruiz-Hussmann, P. Joedecke, S. Abbaszadeh, P.-L. Delafin, C.-T. Weber, and S. Hoerner, "A methodology to capture the single blade loads on a cross-flow tidal turbine flume model," *Proceedings of the European Wave and Tidal Energy Conference*, vol. 15, 2023.